Icarus 295 (2017) 125–139

Contents lists available at ScienceDirect

Icarus

journal homepage: www.elsevier.com/locate/icarus

Clastic patterned ground in Lomonosov crater, Mars: examining fracture controlled formation mechanisms

Alexander M. Barrett[a,*], Matthew R. Balme[a], Manish R. Patel[a,b], Axel Hagermann[a]

[a] Department of Physical Sciences, The Open University, Walton Hall, Milton Keynes, Buckinghamshire MK76AA, UK
[b] Space Science and Technology Department, STFC Rutherford Appleton Laboratory, Chilton, Oxfordshire OX11 0QX, UK

ARTICLE INFO

Article history:
Received 6 February 2017
Revised 2 May 2017
Accepted 5 June 2017
Available online 15 June 2017

Keywords:
Mars
Mars surface

ABSTRACT

The area surrounding Lomonosov crater on Mars has a high density of seemingly organised boulder patterns. These form seemingly sorted polygons and stripes within kilometre scale blockfields, patches of boulder strewn ground which are common across the Martian high latitudes. Several hypotheses have been suggested to explain the formation of clastic patterned ground on Mars. It has been proposed that these structures could have formed through freeze-thaw sorting, or conversely by the interaction of boulders with underlying fracture polygons.

In this investigation a series of sites were examined to evaluate whether boulder patterns appear to be controlled by the distribution of underlying fractures and test the fracture control hypotheses for their formation. It was decided to focus on this suite of mechanisms as they are characterised by a clear morphological relationship, namely the presence of an underlying fracture network which can easily be evaluated over a large area.

It was found that in the majority of examples at these sites did not exhibit fracture control. Although fractures were present at many sites there were very few sites where the fracture network appeared to be controlling the boulder distribution. In general these were not the sites with the best examples of organization, suggesting that the fracture control mechanisms are not the dominant geomorphic process organising the boulders in this area.

1. Introduction

Clastic patterns on Mars are morphologically similar to periglacial patterned ground which is common in cold climate environments on Earth (French, 2007; Washburn, 1956). They have been identified in a variety of places on the Northern Plains of Mars (Balme et al., 2009; Gallagher et al., 2011; Levy et al., 2008a; Mangold, 2005; Orloff et al., 2011). Their distribution is summarised in Section 1.2. These features are particularly common in the area of north-eastern Acidalia Planitia, near Lomonosov crater, and so this region was chosen to be the focus of this investigation. A survey of HiRISE images across the Northern Plains had been completed prior to this work (Barrett, 2014). This region was found to have the highest concentration of potentially sorted sites of any examined, making it most suitable for this analysis. Other putative sorted sites were more isolated, and so did not provide the same variety of features for comparison.

Terrestrial patterned ground develops through the repeated freezing and thawing of the permafrost active layer. This is the upper layer of ice rich soil, up to a metre deep on Earth, which freezes and thaws on a seasonal cycle. This seasonal thaw produces a wet environment and results in a variety of characteristic landforms such as sorted patterned ground. Thus, if Martian clastic patterns are periglacial in origin then they would provide a useful geomorphic marker for locations where thaw has occurred in the geologically recent past.

However, the current climatic conditions on Mars are not favourable for repeated thawing of ground ice due to the extreme cold and low relative humidity of the Martian near surface environment (Kieffer et al., 1992). This may suggest that instances of sorted patterned ground are relict landforms, left over from an era when the climate was more favourable for thawing. However, several alternate mechanisms have been proposed to account for the formation of these patterns without the need for thawing.

Two of these hypotheses suggest different ways in which clastic networks could form through the interaction of metre-scale clasts with an underlying fracture network. In the first hypothesis, clastic material is moved by gravitational slumping into degrading ther-

* Corresponding author.
E-mail address: alexbarrett.malvern@hotmail.com (A.M. Barrett).

http://dx.doi.org/10.1016/j.icarus.2017.06.008

mal contraction fractures (Levy et al., 2008a). In the second, clasts are moved by the opening and closing of nearby fractures in a process known as “boulder ratcheting” (Orloff et al., 2013). These models, which will be collectively referred to as “fracture control” hypotheses, are more fully detailed in Section 1.3.

These mechanisms would potentially allow the formation of sorted clastic patterns under present environmental conditions and would thus dramatically expand the range of environments in which they can develop. Fracture polygons are ubiquitous at high latitudes on Mars and CO_2 frost forms seasonally in this area. This means that clastic patterns which form through fracture control could potential occur anywhere within this environment, rather than requiring a specific microclimate, or the presence of cryobrines as would be the case with patterns which developed through a freeze-thaw mechanism.

In this investigation, examples of clastic networks were studied using HiRISE images (Delamere et al., 2003, 2010; McEwen et al., 2010). These sites were studied to evaluate what proportion of networks had an underlying fracture network and to examine the morphological relationships between the two types of network in locations where both were present.

1.1. Aims and objectives

In this investigation the fracture control hypotheses of gravitational sorting and boulder ratcheting by CO_2 frost are examined to assess the likelihood that they are responsible for the formation of clastic network landforms in the Lomonosov crater region. In locations where both types of network (thermal contraction fracture networks and clastic networks) are collocated, the patterns are compared to determine whether boulder arrangements match those predicted by these models; whether boulders have been transported into polygon troughs through gravitational pull, or are arranged parallel to fracture troughs as a result of boulder ratcheting.

The aim of this study is to test whether the morphologies of the observed clastic networks are influenced or controlled by the arrangement of underlying fractures. A positive result would support the hypothesis that clastic polygon and circle landforms could have formed without the need for freeze-thaw cycles in ice-rich soil. A negative result would leave open the question of how these features formed at this site, since it does not validate the freeze thaw hypothesis.

This study does not attempt to directly assess the alternate, freeze thaw hypothesis for the formation of these features. Fracture control is characterised by clear morphological signatures as described above. The presence or absence of fractures and the relationship between them and overlying clastic networks was easy to assess over large areas. This allowed a thorough examination of this hypothesis across the Lomonosov crater region.

The periglacial freeze thaw mechanism cannot be confirmed by the absence of a fracture network. The characteristic features of this process, such as the presence of excess ice in the subsurface, and the evolution of patterns through repeated phases of frost heaving are harder to evaluate from the large scale geomorphology. This mechanism can be examined using analogue studies to compare the morphology and situation of Martian features to sorted patterned ground on Earth, and by considering the proximity to other putatively thaw related landforms. These methods have been applied to Martian clastic patterns by previous studies (e.g. (Gallagher et al., 2011; Gallagher and Balme, 2011; Hauber et al., 2011a; R. J. Soare et al., 2016). The results of these studies informed the current work, however a direct assessment of the periglacial hypothesis through one or more analogue studies was beyond the scope of this investigation.

1.2. Clastic patterned ground on Earth

Sorted patterned ground is commonly found in periglacial landscapes on Earth. It is common in ice-rich permafrost areas such as the Canadian Arctic, northern Greenland, Iceland and Spitsbergen, as well as in lowland and alpine environments where permafrost has undergone thaw on a seasonal cycle in the geologically recent past (Feuillet et al., 2012; French, 2007; Washburn, 1956).

In these environments, the permafrost active layer freezes and thaws on a seasonal cycle. This process periodically generates areas of soil saturated by liquid water, which then refreeze during colder parts of the year. Freezing fronts propagate through the soil column from colder regions, including the region below the active layer which remains perennially frozen. Ice lenses form within the soil, heaving the surface above. Freezing fronts propagate at different speeds through areas of finer and coarser material. This results in differential frost heave between regions with more fine or coarse material. (e.g. Corte, 1963; Kessler and Werner, 2003; Kessler et al., 2001; Krantz, 1990).

Sorting occurs as a result of the positive feedback created by repeated cycles of differential frost heaving. Sedimentary materials of different sizes respond to heaving to different extents, so they are not displaced by equal amounts (Kessler and Werner, 2003; Matsuoka et al., 2003; Nicholson, 1976). The result is that fine grained material becomes separated from coarser stones and gravel. These separate fine and coarse domains are more susceptible to differential frost heaving than the initial mixed domains, so the process becomes more pronounced with each additional cycle.

Over many seasonal cycles elaborate patterns can develop due to the interaction of coarse and fine domains. In an unconstrained setting a sorted circle would form, where rings of coarse material surround a central fine domain. However the underlying topography can result in elongated circles where material is preferentially displaced downslope. On hillsides these elongated patterns develop into sorted stripes as a result of consistently steeper gradients. The interaction between sorted forms constrains the movement of material resulting in networks of sorted polygons, stripes and labyrinthine structures (Kessler et al., 2001; Krantz, 1990; Washburn, 1973, 1956). Examples of these features are illustrated in Fig. 1. Since periglacial patterned ground results from a freeze-thaw cycle it can only occur in an environment where the upper 50 cm to 1 m of ground ice undergoes repeated thawing, producing an active layer.

1.3. Clastic patterned ground on Mars

Putative clastic patterned ground has been identified in various locations across the Northern Plains of Mars (Balme et al., 2013; Gallagher et al., 2011; Johnsson et al., 2012; Orloff, 2012) as well as at lower latitudes in Elysium Planitia (Balme et al., 2009), and in the Argyre Basin (Banks et al., 2008; Soare et al., 2016). These sites exhibit a variety of morphologies, many of which have similarities to clastic patterned ground on Earth. Organised boulder patterns have been documented both at low latitudes in Elysium Planitia (Balme and Gallagher, 2009), at high latitudes in and around Heimdal crater, near the Phoenix lander site (Gallagher et al., 2011), and across the Vastitas Borealis (Gallagher and Balme, 2011; Orloff et al., 2011).

Many clastic networks are found in proximity to fracture networks, which are ubiquitous at high latitudes on Mars (Gallagher and Balme, 2015; Levy et al., 2010, 2009a, 2008b; Mangold, 2005). These are believed (Mellon, 1997) to form through the thermal contraction cracking of ice-cemented ground as a response to sudden shifts in ground temperature away from sub-zero conditions (Lachenbruch, 1962). They exhibit a range of morphologies similar to those expressed by thermal contraction crack networks on

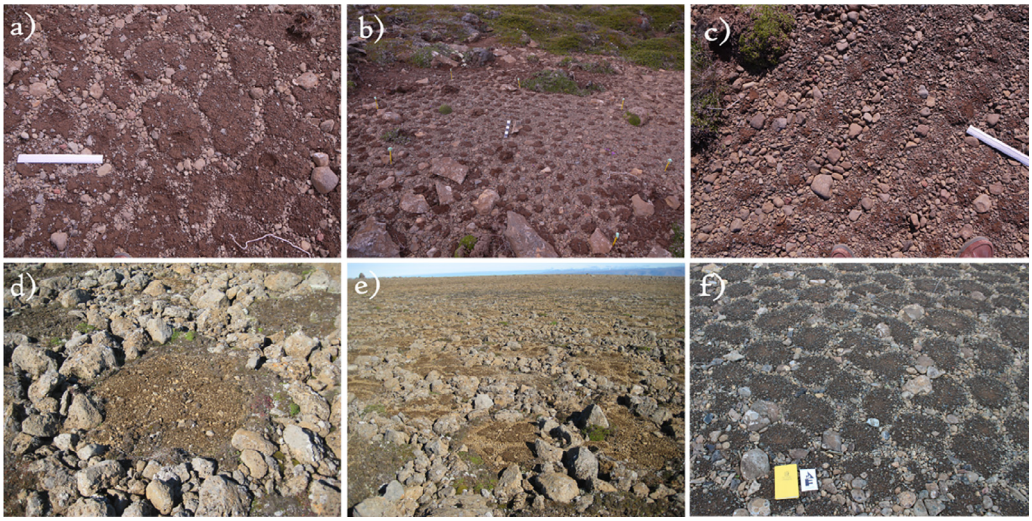

Fig. 1. Examples of sorted patterned ground in Iceland. A variety of different pattern morphologies are illustrated; a) Sorted polygons grade into a discontinuous net, b) Small fine domains surrounded by large coarse areas, c) Stripes of large stones are interspersed by bands of smaller material, d) Metre scale sorted polygon comprised of 10 cm scale coarse material, e) Sorting on multiple scales, centimetre scale patterned ground within metre scale polygons. f) Clear centimetre scale polygonal net. The ruler in frames a–c is 30 cm long, the circles in d and e are approximately 1 m in diameter and the notebook in f is approximately 15 cm in length. (Photos a–c by Chris Barrett, d and e by Alex Barrett, f by Susan Conway and Andrew Wilson).

Earth (Haltigin et al., 2012; Johnsson et al., 2012; Levy et al., 2010; Rossi et al., 2011; Soare et al., 2011; Ulrich et al., 2011). Fracture patterns have frequently been found in proximity to other putative periglacial landforms (Hauber et al., 2011b; Johnsson et al., 2012; Ulrich et al., 2012). In particular the scalloped depressions which are common at mid latitudes in Utopia Plainitia are often superposed by fracture networks (Haltigin et al., 2014; Séjourné et al., 2011; Soare et al., 2014; Ulrich et al., 2012). Martian gullies which have been suggested to result from thawing frequently occur in proximity to polygonal structures (Levy et al., 2009b; Soare et al., 2014). Mounds which have been hypothesised to be analogous to terrestrial pingos also frequently occur on fractured terrain (Dundas and McEwen, 2010; Soare et al., 2005).

There are a number of locations where clastic patterns seem to be influenced by the underlying arrangement of fracture networks (Levy et al., 2010; Orloff et al., 2011). Consequently, it is possible that many clastic patterns are the result of interactions between the boulders and the fracture networks (Orloff et al., 2013).

1.4. Possible formation mechanisms for Martian patterned ground

Several hypotheses have been proposed to explain the formation of the boulder patterns on Mars. These fall into two main categories: freeze-thaw sorting of clastic material, and the interaction of boulders with fracture networks. The latter could occur through either gravitational sorting (Levy et al., 2010, 2008a; Mellon et al., 2008) or more exotic processes involving ratcheting of boulders trapped in carbon dioxide frost (Orloff et al., 2013).

1.4.1. Boulder ratcheting

In the boulder ratcheting model of Orloff et al., (2013) it has been suggested that apparently sorted, clastic networks could result from the interaction of boulders with a layer of carbon dioxide frost. In the winter, the temperatures drop and CO_2 from the atmosphere condenses to form a slab of frost up to a metre deep, trapping loose boulders.

These boulders are locked in place by the CO_2 frost and so are not moved when a thermal contraction fracture opens in the ground due to the change in temperature. The ground beneath the boulder, in contrast, moves away from the fracture with respect to the CO_2 slab. When the temperature rises again, it triggers the sublimation of the carbon dioxide frost and the closing of the contraction cracks. The boulders are now free to move with the ground beneath them and so there will be a small net migration of boulders towards the contraction cracks for each annual cycle of CO_2 deposition and thermal contraction crack opening/closing. Over many such cycles, Orloff et al., (2013) suggest that this results in the formation of a clastic net parallel to the underlying fracture net. It should be noted that boulders are also seen lying within fracture troughs at some sites in Orloff's study area, suggesting either that this mechanism results such a pattern as well, or that the gravitational slumping mechanisms can occur concurrently. The later seems most likely, as gravitational slumping can occur anywhere where a fracture is present.

Since the climate of modern day Mars is very cold and dry, hypotheses such as this, which do not require thawing of ground ice, are very interesting as they would potentially allow these features to form in the present day. Thaw related processes frequently rely on a favourable microclimate, or past period when the climate was more suitable for pattern formation. Boulder ratcheting could potentially be more ubiquitous on present day Mars. However, the boulder ratcheting hypothesis involves a process with no terrestrial analogue, and so additional evidence, from experimental or modelling studies would be required to demonstrate that this mechanism would produce the observed result.

1.4.2. Gravitational sorting

Boulder patterns in the Martian high latitudes could result from the gravitational sorting of large clastic material (Levy et al., 2010, 2008a; Mellon et al., 2008). In this model, the presence of degraded fracture polygons can result in the slumping and rolling of boulders into the topographic lows, producing clastic polygons (Levy et al., 2008a). This hypothesis would neither require the action of freeze thaw processes nor an interaction of boulders with carbon dioxide frost. Consequently, it would provide a simpler mechanism to explain the observed structures at sites where fracture control is apparent. On the other hand, it is not clear how irregular boulders would be able to move on the low slopes seen on the shoulders of thermal contraction cracks.

1.4.3. Periglacial sorting

On Earth, sorted patterns result from the cyclical freezing and thawing of the permafrost active layer. It has been suggested (Gallagher and Balme, 2011) that Martian clastic networks could have formed through similar processes. Such landforms could be relict features, which formed at a time when the climate of Mars was more favourable to thaw, or they could form in unusual microclimates where the temperature rises above the freezing point of water on a regular basis. It is further possible that the presence of brines such as magnesium perchlorate in the Martian near surface could depress the freezing point and allow thawing to occur despite the low temperatures on Mars (Hecht, 2002; Marion et al., 2010). The recent detection of hydrated salts in the vicinity of recurring slope lineae (RSL) in the equatorial regions of Mars by Ojha et al., (2015) lends some weight to this hypothesis, since these are thought to form on present day Mars as liquid flows of brine or water on steep slopes.

The periglacial hypothesis is difficult to test without in situ observations. Similarities in morphology and situation to terrestrial features can provide circumstantial evidence for a periglacial origin, but direct observation of freezing and thawing is not possible using the remote sensing images we currently have available.

It is theoretically possible that changes in the arrangement of clasts could be observed in iterative HiRISE image, and that this might support one or other formation mechanism. However complex clastic patterns take a long time to evolve, and so significant changes would not be expected in the relatively short time series that is currently available. There is also a general lack of repeat observations by HiRISE in this area. Critically remote sensing images are not capable of detecting the small scale elevation changes associated with frost heaving, or the presence or absence of subsurface ice lenses, which would be direct evidence of freeze-thaw sorting.

The presence of perchlorate salts in proximity to a sorted site would support this hypothesis, as it could indicate that thaw is practical at that location. Such identification might be possible using orbital reflectance spectroscopy techniques, as has been done for very recently formed salt deposits near RSL (Ojha et al., 2015). However, given Mars' annual dust deposition rates (Aharonson et al., 2003; Landis and Jenkins, 2000), and given that orbital remote sensing reflectance spectroscopy detection of any minerals on Mars can be prevented by the presence of very thin dust layers (Ruff, 2002), it is perhaps unlikely that such observations could easily be made unless such salts were formed extremely recently.

2. Methods

2.1. Study area

Located at 64.9°N, 9.3°W, Lomonosov crater is a 150 km diameter impact structure with a ~ 100 km radius ejecta blanket. It is surrounded by the generally low-lying plains of the Vastitas Borealis. The region of north-eastern Acidalia Planitia in the vicinity of Lomonosov crater has a very dense concentration of clastic networks compared to most of the Northern Plains. The Lomonosov region is characterized by numerous blockfields which range in size from a few hundred metres to about a kilometre across. These boulder patches are the densest concentrations of boulders in the area. Many form "boulder halos"; rings of rubbly material which surround small or buried impact craters (Levy et al., 2008a; Orloff et al., 2011).

In many patches, the metre-scale clasts do not appear to be randomly distributed. Instead they form lines and arcs of clasts. In some cases, these appear to be part of a discontinuous network, with network elements having diameters of around 20–50 m. Many of these structures appear to be morphologically similar to the sorted polygons found in terrestrial periglacial environments, albeit on a much larger scale.

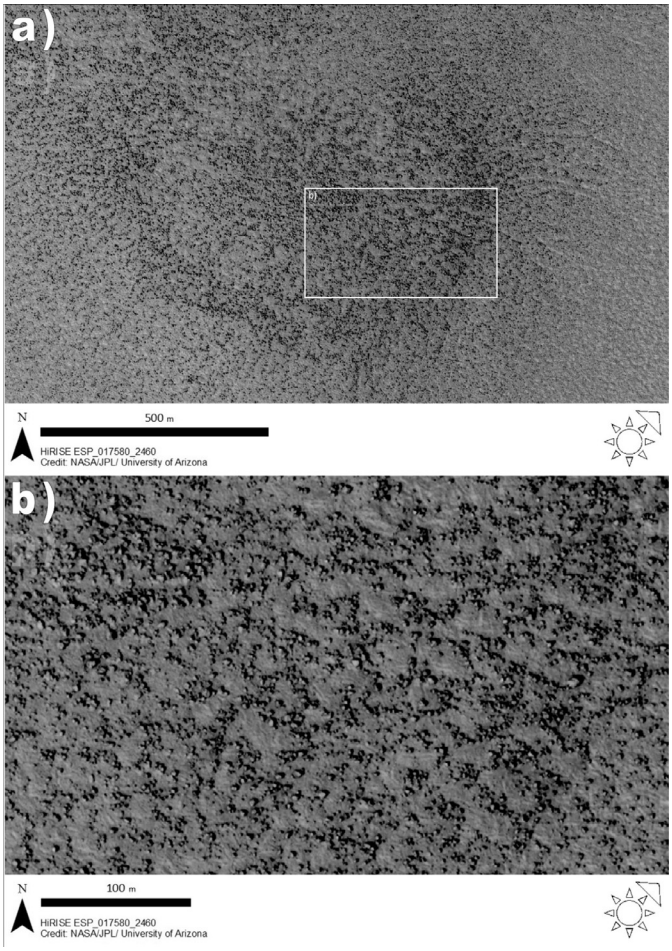

Fig. 2. a) A kilometre scale boulder patch in HiRISE image ESP_017980_2460 in the vicinity of Lomonosov crater. b) Organised boulder network at this site. Sun direction is indicated for both images.

It is likely that these clusters of boulders were emplaced through ejection of fragmented material from their associated impact craters (Levy et al., 2008a) or perhaps by fragmentation of the local bedrock and exposure by erosion. The boulders were distributed around the crater, presumably in a somewhat random distribution, and later arranged by other processes to form the observed patterns (Levy et al., 2010, 2008a; Mellon et al., 2008; Orloff et al., 2011, 2013; Orloff, 2012).

An example of a boulder patch is illustrated in Fig. 2. Some boulder fields are underlain by fracture patterns, while others are on smooth ground without any visible fractures. No examples of sorted patterned ground have been found outside the boulder patches, where clasts are more sparsely distributed.

147 boulder clusters were examined across the 17 HiRISE images within 500 km of Lomonosov crater. Five of these images cover sections of the crater interior while 12 are located on the surrounding plains. Table 1 lists the HiRISE images examined in this area. The distribution of images adjacent to Lomonosov crater is shown in Fig. 3.

2.2. Surveying procedure

Boulder patches are clearly visible in Context Camera (CTX) and High Resolution Stereo Camera (HRSC) images, however only sites with HiRISE images were chosen for this study, as it proved

Table 1
HiRISE images examined.

Image	Location		Latitude	Longitude	Solar longitude
PSP_001520_2470	Exterior	West of crater	66.575°	332.881°	139.4°, Summer
PSP_007440_2455	Interior	Crater interior	64.987°	351.008°	37.6°, Spring
PSP_010051_2435	Exterior	West of crater	63.094°	339.264°	128.6°, Summer
PSP_010644_2455	Interior	Crater interior	65.264°	349.498°	151.5°, Summer
TRA_000846_2475	Exterior	East of crater	67.069°	0.012°	114.4°, Summer
ESP_017079_2410	Exterior	South of crater	60.458°	348.761°	66.0°, Spring
ESP_017131_2485	Exterior	East of crater	68.041°	6.672°	67.7°, Spring
ESP_017580_2460	Interior	North wall	65.672°	350.288°	83.0°, Spring
ESP_017632_2475	Exterior	East of crater	67.054°	9.226°	84.8°, Spring
ESP_017685_2490	Exterior	East of crater	68.743°	−1.182°	86.6°, Spring
ESP_019900_2470	Exterior	East of crater	66.925°	9.267°	169.7°, Summer
ESP_023738_2415	Exterior	South of crater	61.061°	348.710°	347.6°, Winter
ESP_025294_2415	Exterior	South of crater	61.426°	348.533°	45.4°, Spring
ESP_025769_2435	Exterior	West of crater	63.168°	339.345°	61.7°, Spring
ESP_026441_2460	Interior	East Wall	65.561°	352.299°	84.6°, Spring
ESP_026850_2475	Exterior	North West	67.343°	345.811°	98.7°, Summer
ESP_027918_2455	Interior	East Wall	65.061°	351.573°	37.6°, Spring

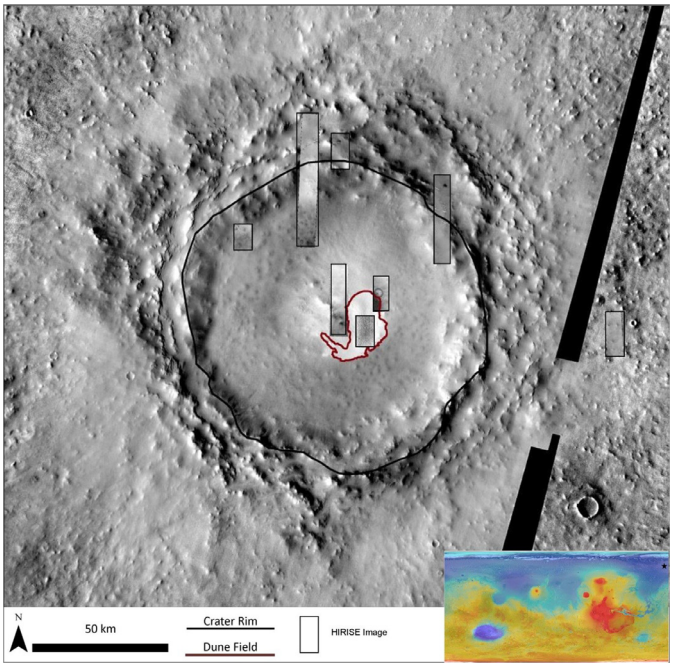

Fig. 3. Map of Lomonosov crater showing the location of the crater rim and the extent of the central dune field. The distribution of HiRISE images across the crater interior is shown. Right to left across north crater wall: PSP_010644_2455, ESP_017580_2460, PSP_010011_2460, ESP_026441_2460. Crater centre: PSP_007440_2455, PSP_002047_2450, ESP_027918_2455. To east of crater: ESP_027153_2455 (Credit: NASA/JPL/University of Arizona. Background: THEMIS IR day 100 m global mosaic (Christensen et al., 2010.) with MOLA global topographic map for context (Smith et al., 2001)).

unreliable to determine whether organization was present using lower resolution images. In a HiRISE image (25 cm/pixel) individual boulders can be distinguished and an assessment can be made of whether any degree of organisation of the clasts is present.

All boulder patches within the study area were identified and those covered by HiRISE images were assessed for a number of parameters. Firstly, the presence and quality of a sorted net was assessed. This was done using the semi-quantitative scale described in Section 2.3, below. In order to confirm that this assessment was reliable, examples from across the study area were digitized into a point shapefile using ArcGIS software by adding a single point to represent each discernible clast. An average nearest neighbour analysis was then conducted on these point shapefiles to determine whether the distribution of boulders was significantly different from a random distribution.

The presence of an underlying fracture pattern was determined by visual inspection of the entire area covered by the boulder patch. If fractures were present anywhere within the patch then it was considered to have the potential for fracture control and was examined more closely. The likelihood that the sorted net was related to the underlying fracture pattern was assessed using the following criteria:

- The two networks were present in the same parts of the image,
- The boulder network appeared to mirror the fracture network,
- Boulders were present within fractures.

2.3. Sorting classification

A semi-quantitative scale was designed to classify the degree to which organization was present in any given boulder patch. The degree of sorting at each of these sites was ranked between zero (no evidence of organisation) and five (exhibiting a distinct sorted pattern). The criteria are summarised below (Table 2).

In order to perform this classification, the observed features were compared to type examples from previous studies on this subject, in particular from Gallagher et al. (2011b). A grade was chosen based on the arrangement of clasts and the similarity of the features to the type examples. Sites which were classified as falling between grades zero to two are considered to lack patterned ground. There may be a small amount of clustering of clasts, but not sufficient to suggest that the arrangement is indicative of an underlying process. Sites with grade three may suggest that a sorting process is at work but remains uncertain, while those classified as grades four or five are considered to be organized due to geomorphic processes.

2.4. Nearest neighbour analysis

Assessing by eye whether a pattern is present within an arrangement of clasts is inescapably subjective. Consequently, this semi-quantitative assessment was tested using an average nearest neighbour analysis approach to determine whether sites which had been rated as being organised were in fact significantly different from a random distribution.

The nearest neighbour analysis (Clark and Evans, 1954) is a statistical technique which assesses whether there is a pattern in a population of points by comparing the distances between each point and its nearest neighbours to the expected distance based on a hypothetical random pattern. The resulting ratio (R) indicates

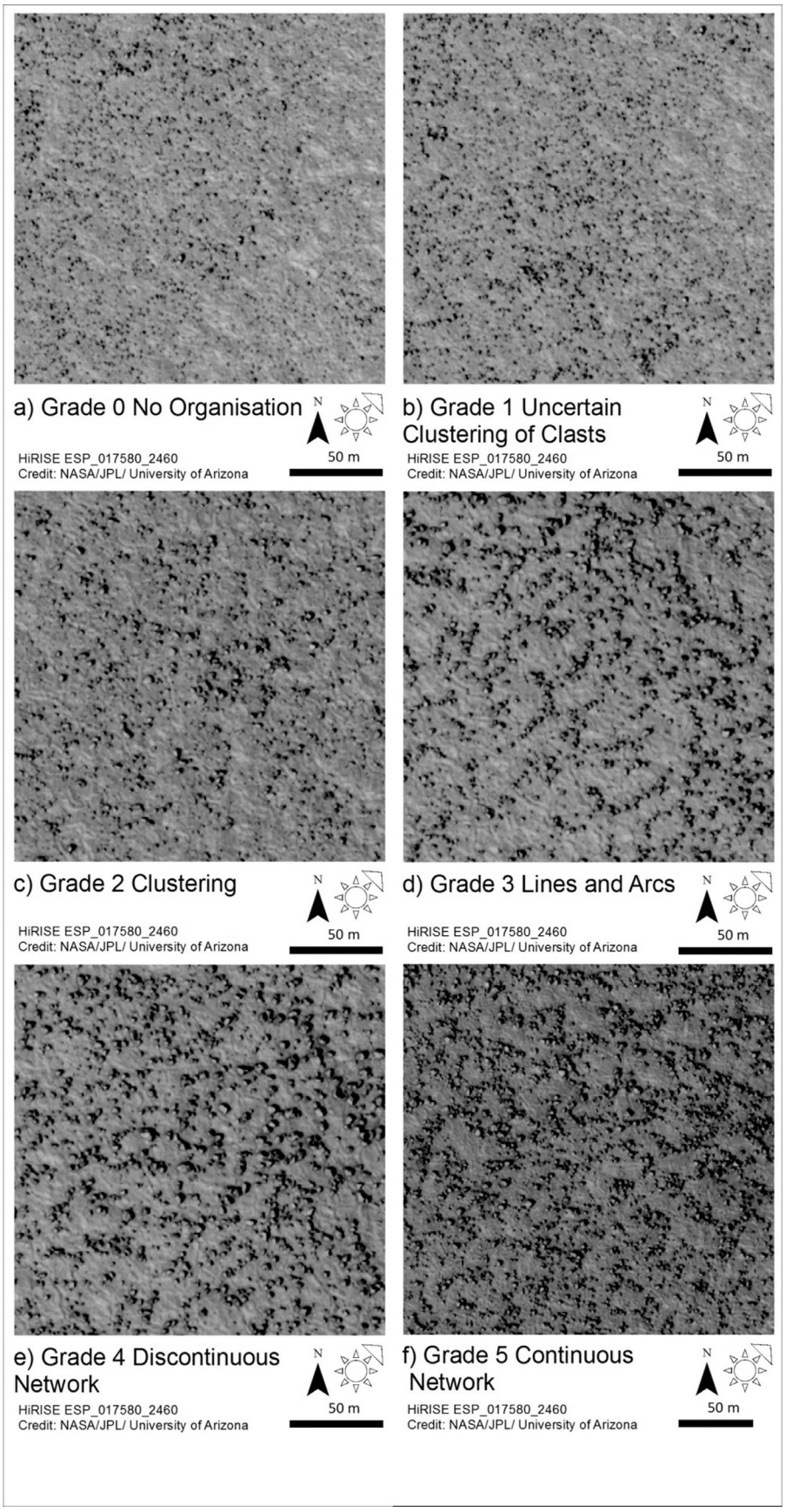

Fig. 4. Illustration of clastic patterns of each sorting grade; a) Grade 0, no evidence of sorting, b) grade 1, uncertain organization, c) grade 2 possible clustering of clasts, d) grade 3, clear lines and arcs, e) grade 4, discontinuous net, f) grade 5, continuous network, note that only small areas of grade 5 terrain occur within larger patches of discontinuous networks.

Table 2
Classification system for patterned ground observations.

Grade	Description	Criteria for classification
Zero	No evidence of organisation	Boulders are scattered across the image in a seemingly random distribution and no lines or clusters of clasts are apparent.
One	Uncertain clustering	There may be some clustering or alignment of clasts but whether a pattern is present remains highly uncertain.
Two	Clustering of clasts	There are some areas where clasts appear to be clustered or coaligned, but they do not form a clear pattern.
Three	Clear lines and arcs	Boulders are arranged into lines separated by reasonably clear spaces but do not form coherent polygons.
Four	Discontinuous network	Lines of clasts are common and most clasts appear to fit the edges of a polygonal net, even if that net is not continuous.
Five	Continuous network	Clasts form clear sorted stripes and polygons similar to those seen in terrestrial periglacial environments and examples from the Mars periglacial literature.

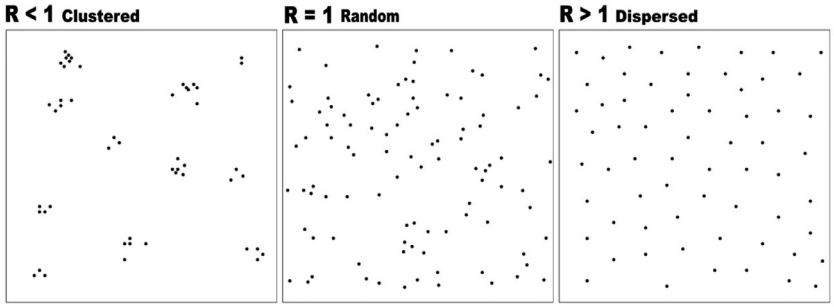

Fig. 5. Interpretation of average nearest neighbour analysis. Dispersed patterns return R values greater than one while clustered patterns produce lower R values.

Table 3
Interpretation of R values

R value	Pattern
0	Collocated
< 1	Clustered
1	Random
> 1	Dispersed
2	Square lattice
2.149	Triangular lattice

whether the features under analysis are randomly distributed, clustered, or dispersed. An R value of zero indicates that all points plot in the same location. R values between zero and one indicate a clustered arrangement while R values greater than one suggest that the arrangement of points is significantly dispersed. The theoretical maximum dispersion is R= 2.149, indicating that the points are arranged in a triangular lattice. Table 3 describes the range of R values that can be returned. Fig. 5 shows the types of patterns these values reflect.

The null hypothesis for this test is that the distribution of points is spatially random and consequently, has an R-value of one. The probability that this is the case is given by the p-value. Low p-values suggest that the distribution is very unlikely to be random, and that the distribution of the points has been influenced by some underlying process. A z-score gives the standard deviation of the result. A z-score between −1.96 and 1.96 indicates that the pattern is not significantly different from a random distribution at a confidence of 0.05. A z-score less than −1.96 or greater than 1.94 returns a significantly clustered or dispersed result respectively; the null hypothesis can thus be rejected. Significance can be assessed either using the p-value or the z-score. Variations on the nearest neighbour approach have previously been applied to assessing randomness arrangements of fracture polygons (e.g. Dutilleul et al., 2009; Haltigin et al., 2012).

When the method was tested using examples of terrestrial patterned ground it was found that the resolution of the image strongly affected the result (Barrett, 2014). High resolution images, taken in-situ, preserved all of the detail of the pattern, so the clustering of clasts within a coarse domain could be detected by the nearest neighbour analysis. In remote sensing images, this was not the case. In air photos and satellite images (similar to those available for Mars) a strongly dispersed result was generally returned. This is due to the appearance of only the coarse domain in these images. It is impossible to see the clustering of smaller clasts within the coarse domains and so only the discontinuous network of very large clasts can be detected. Albedo differences that reflect the underlying pattern do not inform the test, only discrete clasts.

Although the occurrence of boulders large enough to be resolved is largely random, their distribution around the feature is not. In terrestrial sorted patterned ground, larger clasts are distributed into a polygonal lattice around open fine domains. The large boulders are seen by the algorithm as being spread out around the fine domains and so it returns a dispersed result. Organisation can still be detected in these features, despite the fact that most of the detail is below the resolution of the image. It is thus expected that the nearest neighbour analysis will return a dispersed result in most cases where organization appears to be present.

The patterns of boulders at twenty-five sites across the Lomonosov Region were digitized using ArcGIS. A variety of sites that had been classified with different grades of sorting were examined, as well as (i) transitional sites which were less easy to classify, and (ii) some locations where no pattern was believed to be present, and the boulders appeared randomly distributed. Several representative sites for each category of the classification system were selected so that this analysis would be applied to all varieties of patterned ground described in the previous section.

Three sites with no appreciable pattern were selected, along with two grade one sites, where uncertain clustering was present. A site which was transitional between grades one and two was also selected. Five grade two sites were examined, including examples where clustering was less certain, and some at the higher end of grade two which almost appeared to have coherent lines and arcs. A similar variety of grade three sites were selected, including a transitional site where the lines and arcs were almost sufficient to be classified as a discontinuous network. Five grade four sites were chosen, as were the clastic stripes illustrated in Fig. 9. This was the only grade five site where a pattern extended over a large

Table 4
Results of nearest neighbour analysis of sorted patterned ground in and around Lomonosov crater.

Sorting Grade	Type	Result	Site ID	Mean distance observed	Expected	R-value	z-score	p-value
0	No pattern	Random	Site 4	0.000072	0.000072	1.00	0.14	0.89
0	No pattern	Clustered	Site 6	0.000077	0.000082	0.94	−2.89	0.00
0	No pattern	Clustered	Site 24	0.000107	0.000114	0.95	−3.39	0.00
1	Net	Clustered	Site 5	0.000092	0.000097	0.95	−3.39	0.00
1	Net	Dispersed	Site 25	0.000083	0.00008	1.04	2.57	0.01
1-2 transitional	Net	Random	Site 7	0.000064	0.000066	0.98	−1.12	0.26
Low 2	Net	Random	Site 18	0.000067	0.000065	1.03	1.57	0.12
2	Rubble piles	Random	Site 17	0.000065	0.000065	1.01	0.66	0.51
2	Rubble piles	Random	Site 22	0.000068	0.000067	1.02	1.49	0.14
2	Net	Dispersed	Site 23	0.00007	0.000067	1.04	2.97	0.00
High 2	Net	Dispersed	Site 13	0.000118	0.000111	1.07	7.16	0.00
2-3 transitional	Net	Dispersed	Site 10	0.000079	0.000068	1.16	8.57	0.00
Low 3	Net	Random	Site 9	0.000098	0.000096	1.02	1.31	0.19
Low 3	Net	Clustered	Site 14	0.000121	0.000305	0.40	−47.43	0.00
3	Stripes	Clustered	Site 15	0.00015	0.000205	0.73	−24.73	0.00
3	Net	Clustered	Site 16	0.006309	0.053979	0.12	−84.32	0.00
High 3	Net	Clustered	Site 12	0.000089	0.00009	0.99	−1.67	0.10
High 3	Net	Dispersed	Site 20	0.000054	0.000049	1.11	7.72	0.00
3-4 transitional	Net	Dispersed	Site 8	0.00007	0.000059	1.19	13.62	0.00
4	Net	Dispersed	Site 1	0.000081	0.000069	1.17	10.67	0.00
4	Net	Dispersed	Site 2	0.000086	0.000076	1.14	11.50	0.00
4	Net	Dispersed	Site 3	0.000067	0.000062	1.08	6.53	0.00
4	Net	Dispersed	Site 19	0.000064	0.000061	1.05	4.22	0.00
4	Net	Dispersed	Site 21	0.000068	0.000066	1.03	1.93	0.05
5	Stripes	Clustered	Site 11	0.000036	0.000054	0.66	−24.56	0.00

Table 5
Summary of sites and images featuring patterns of each sorting grade.

Grade	Description	Sites	% of Sites	Images	% of Images
0	No evidence of organisation	26	17.69	6	13.95
1	Uncertain clustering	32	21.77	7	16.28
2	Clustering of clasts	38	25.85	13	30.23
3	Clear lines and arcs	35	23.81	12	27.91
4	Discontinuous net	15	10.20	4	9.30
5	Clear pattern	1	0.68	1	2.33

enough area to be used for the nearest neighbour analysis. Most grade five networks consist of smaller patches with a continuous pattern within larger discontinuous nets. This variety of sites provides a good range of different feature types, and examples which are characteristic of most of the varieties observed during the survey (Fig. 4).

3. Results

3.1. Results of the nearest neighbour analysis

It was found that most of the sites which appeared highly sorted, exhibiting a discontinuous net and scoring four on the classification scheme, yielded results suggesting that they were strongly dispersed. All of the grade four sites returned a dispersed result, as did the grade 3 site classified as being transitional with grade four. One other grade 3 site returned a dispersed result as did several of the higher end grade two sites (although this could be due to the low boulder density at some of these sites rather than the presence of a stronger sorting pattern). Most of the other grade three sites indicated clustering of boulders. Only one low grade 3 site returned a randomly distributed result (Tables 4 and 5).

The low grade 2 sites, where very little organisation was observed in the visual survey, generally returned a random classification. Both sites which were selected for having apparent rubble piles returned a “random” result. This is probably because many small clasts surround the denser concentrations of clasts and these randomly distributed clasts are identified as the average structure across these areas rather than the small clusters. If different sizes of boulder could be given a different weighting, then these sites might return a different result.

Both sites with stripes returned clustered results due to the arrangement of clasts within the stripes. This was the expected result for these features. Most of the sites which were selected for their lack of an apparent pattern (grades zero and one) returned a “clustered” result, with a few found to be “randomly” distributed.

There is a clear difference between sites graded as having high organization, which have a consistently dispersed pattern, and low-graded sites with a random or clustered result. These results would seem to suggest that the “background” arrangement of clasts is generally either random or clustered depending on the site. Sites with higher sorting grades do display clast arrangements that are significantly different to those expected from randomly emplaced clasts. This suggests that an underlying geomorphological process is likely to be responsible for the apparent structure in their emplacement, rather than it being the result of chance. The fact that similar patterns occur across the region, and return similar results in this test, reinforces this conclusion. This also suggests that the semi-quantitative grading is largely reliable as a means of assessing the organization at a given site.

3.2. Distribution of clastic patterns

Fig. 6 shows the distribution of patterns of different sorting grades. The only site with grade 5 sorting across a large area occurs in image ESP_017131_2485 where numerous clastic stripes are seen (Fig. 9). 15 boulder patches contain features classified as discontinuous nets (grade 4 sorting.) Several of these are located in the two HiRISE images covering the west of the Lomonosov crater floor

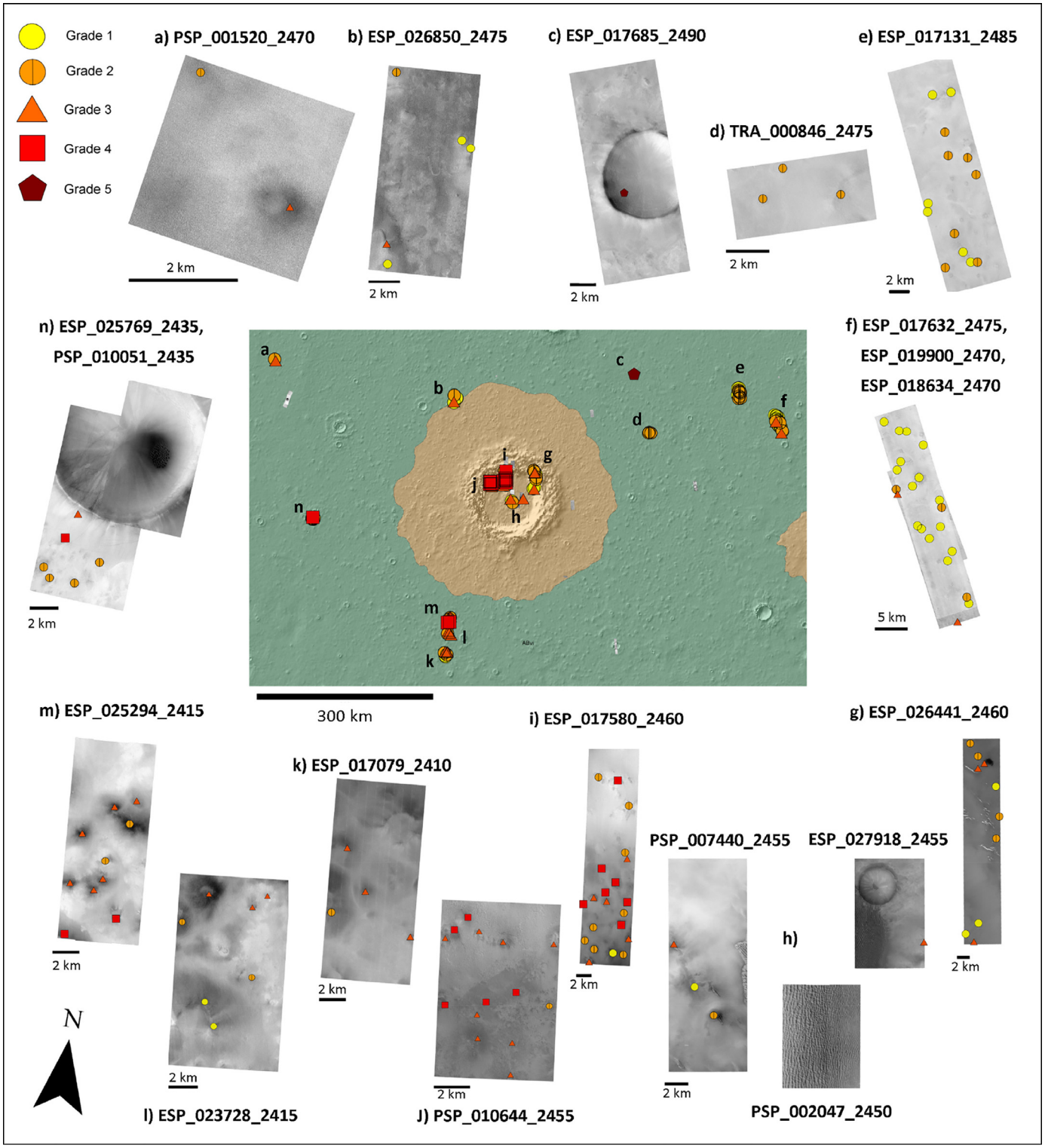

Fig. 6. Results of the boulder patch classification. Each inset shows the distribution of graded features within one or more HiRISE images (NASA/JPL/University of Arizona). The central image shows site locations overlain on the geological map of the Martian Northern Plains (Tanaka et al., 2005), which illustrates the extent of the Lomonosov crater ejecta blanket. 17 Images exhibit features.

(ESP_017580_2460 and PSP_010644_2455). Grade 4 sorting also occurs in ESP_025294_2415, located to the south of Lomonosov crater, and in PSP_010051_2435, to the far west of Lomonosov. These five images are considered to be most likely to contain evidence of organised, clastic, patterned ground.

Thirty-five sites (23.8% of total) exhibit clear lines of clasts (grade 3) and so may be evidence of a partially developed clastic network. However 26 sites (17.69% of total) show no evidence of organisation and 32 sites (21.77%) have uncertain clustering but no clear pattern, giving a total of 58 sites (39.46%) where sorting is unlikely to be present.

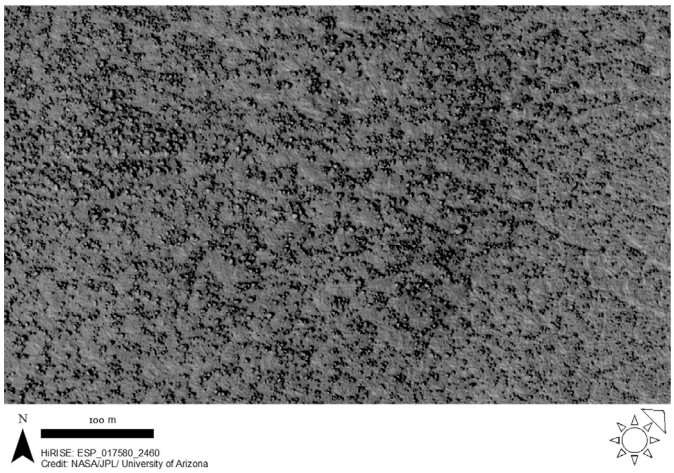

Fig. 7. Possible sorted network on the floor of Lomonosov crater. Lines of clasts and discontinuous polygons in HiRISE image ESP_017580_2460.

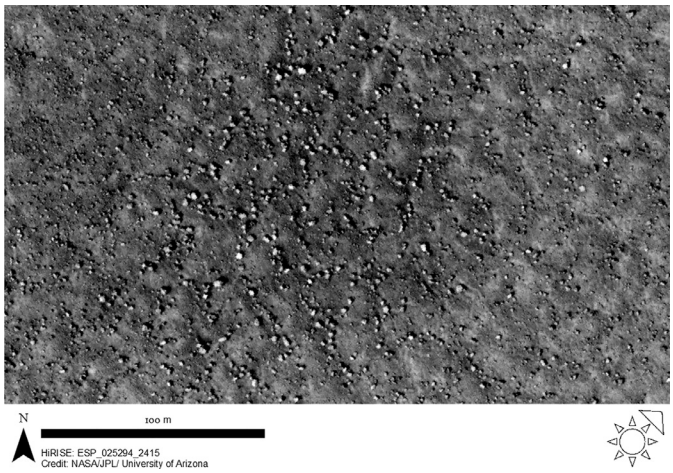

Fig. 8. Net of less dense discontinuous polygons in HiRISE image ESP_025294_2415, covering flat ground to the south of Lomonosov crater.

3.3. Examples of clastic patterns

A variety of different features were observed during this investigation. Most locations that exhibit a high likelihood of sorting consist of patches of discontinuous polygonal networks. However, a few locations were found with different types of patterned ground: two sites contain possible clastic stripes, and several patches of rubble piles were also observed.

Rubble piles are frequently found on Mars, in areas classified as "basketball terrain" due to their stippled appearance in low resolution images (Malin and Edgett, 2001; Mellon et al., 2008). They often overlie fracture polygons. These rubble piles are morphologically similar to sorted islands, which occur in areas of patterned ground on Earth. It is thus possible that they are an expression of the same process which causes clustering of clasts in polygonally patterned areas. Sorted islands, along with labyrinthine arrangements of clasts result from the interaction of polygon coarse domains (Kessler and Werner, 2003).

Clastic stripes (Washburn, 1956)are often found in proximity to sorted polygons on Earth, and form through related processes. They result from the elongation of sorted polygons in the direction of an underlying slope and are thus usually found on hillsides, whereas the more circular polygons occur on flatter ground(e.g. Kessler et al., 2001; Kessler and Werner, 2003). The stripe examples are more likely to be associated with the polygon networks, as they are often found in the same general areas. Rubble piles occur over a wider range and are not always coincident. It was nonetheless thus decided to include these features in the survey.

The polygonal sites are the focus of this investigation, since these were most numerous, and were most likely to have been influenced by fracture patterns. Figs. 7 through 9 illustrate a variety of morphologies that were observed.

HiRISE image ESP_017580_2460 overlaps the northern wall of Lomonosov crater. This image contains 21 boulder clusters, all of which show some form of clast organization, with the highest sorting grade found in the image being 3. In several areas across this image boulders are seen to be grouped into lines and arcs. In a few cases, they form regions of clear ground surrounded by discontinuous lines and clusters of metre scale boulders (Fig. 7). Similar structures can be found in HiRISE image PSP_010644_2455, covering the crater interior just to the west of the site detailed in Fig. 7. Again, clear areas of ground are enclosed by semi-polygons of larger clastic material. Very few areas are completely enclosed, but all 14 boulder patches in this area seem to exhibit some form of organisation (grade 4 in some areas).

A few more discontinuous nets can be found in image PSP_007440_2455 near the centre of Lomonosov crater. As with the other sites, several fields of boulders can be seen. Here larger, ~ 4 m diameter, boulders appear to be arranged into a polygonal pattern but the clear areas are much smaller relative to the size of the clasts, making it harder to be certain that this isn't a random arrangement which just appears organised in places.

Possible sorting is not confined to the interior of Lomonosov crater, similar boulder halos and rubble fields occur across the region. Several images to the south of Lomonosov crater exhibit possible polygons. Image ESP_025294_2415 (Fig. 8) exhibits discontinuous nets. Here, thin lines of metre-scale boulders are more spread out, but seem to enclose open areas and in some cases are accompanied by a slight change in albedo below the clastic lines. Whether this is due to changes in the underlying material, the presence of sub-pixel scale materials, or is the result of the boulders shadowing the ground around them is uncertain. All ten boulder patches within this image exhibit possible sorting and the highest grade found in this image is grade four.

Image ESP_017685_2490 (Fig. 9) covers a medium-sized impact crater where clear clastic stripes can be seen across a wide swath of the crater wall. Running from the rim of the crater down into the interior, these features overlay a net of fracture polygons and are also located within a series of light and dark bands: the ground beneath the clasts seems to be darker, while lighter ground is found between the stripes. This could indicate the presence of sub-pixel scale clasts. This site contains the best examples of organization of clasts found within the survey. The stripes appear to grade into more polygonal structures high up on the crater wall towards the west of the image. Near the centre of the image, the stripes merge into a labyrinthine pattern that covers much of the crater floor. There is a clear fracture pattern in this area. However, the arrangement of the clasts into parallel stripes does not match the underlying fracture distribution, which is polygonal in nature. Similar observations were made by Gallagher et al., (2011) in Heimdal crater, where clastic stripes and lobate structures were observed on the crater wall but did not always align with nearby fracture patterns. Johnsson et al., 2012 report similar features.

4. Analysis

4.1. Testing the fracture control hypotheses

If the hypothesis that the organisation of clasts is controlled by underlying fracture patterns is correct then the observed or-

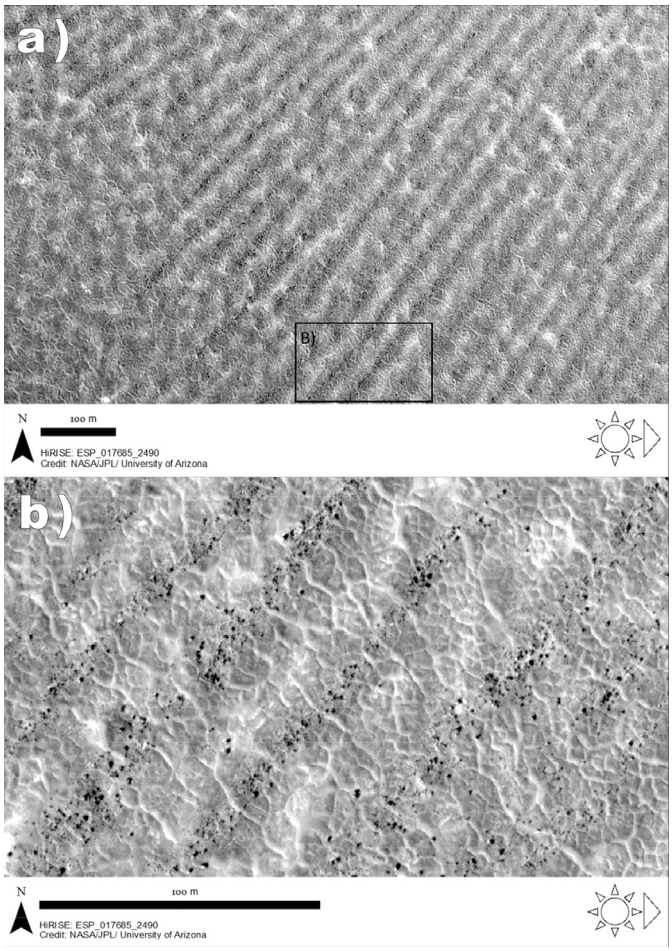

Fig. 9. Small crater in ESP_017685_2490 to the North East of Lomonosov crater. a) The southern wall exhibits alternating bands of dark and bright material. b) Detailed view of clastic stripes.

ganized clastic patterns can be expected to occur on terrain containing well-developed fracture networks, and the distribution of clasts should follow the pattern of the fractures. Consequently, it is possible to assess whether the patterns of clast organization in a sample region appear to be fracture controlled, or whether the organisation of clasts appears to be independent of any thermal contraction polygons.

Fracture patterns are found in 13 out of the 17 HiRISE images surveyed. Fractures are much less common in the images covering the crater interior, than those beyond the crater walls. Very faint fractures can be seen at a few sites, but most boulder patches within Lomonosov crater itself do not overlay fracture nets at all. Images covering the plains beyond the ejecta of Lomonosov crater exhibit more pronounced fracture networks. All 147 boulder patches were assessed independently to determine whether they exhibited fracture control. The results are shown in Table 6.

Fractures are clearly present in 85 of the 147 boulder patches and are tentatively identified in a further seven. Fifty-five boulder patch sites definitely do not exhibit fractures. Of the sites where fractures can be found, only 21 show a relationship between the arrangement of clasts and the underlying fracture network. A further 35 sites have an uncertain relationship, in which it is not clear whether the organisation of clasts mirrors that of an underlying fracture net. Even if the presence of a fracture net controls the organisation of boulders at these sites there remain 91 sites where there is no link between the two, either due to the absence of fractures or the absence of a clear relationship between the patterns.

Table 7 summarises the results for each HiRISE image considered in the survey. The number of boulder clusters within an image and the number that exhibit organisation are listed. The presence or absence of fractures is then stated, as any relationship between clasts and fractures is described.

The presence or absence of an underlying fracture net was also filtered against the sorting grade classifications, to assess whether the presence of an underlying fracture net appeared to be responsible for the degree of boulder organisation at these sites. Table 8 summarises the number of sites of each sorting grade, with and without fractures, and the number of sites which appear to exhibit fracture control. In cases where the number of sites with or without fractures and with or without fracture control do not add up to the total, it is because sites where a fracture net is uncertain have not been counted.

It can be seen that the sites without fractures generally have a higher sorting grade than those with fractures, while the sites where fractures are present, but unrelated, are also correlated with higher sorting grades than sites where there does seem to be a relationship.

In many cases, the sites where the two network types appear to be related consist of clusters of boulders separated by the fractures, rather than lines of clasts following fracture lines, or discontinuous nets superimposed on the fracture pattern. This morphology is to be expected anywhere a fracture network cross-cuts a boulder field, and so is not indicative of the boulder ratcheting processes proposed by Orloff et al., (2013). It is also not consistent with the gravitational sorting mechanism in which clasts are concentrated by slumping into polygon- bounding troughs (Levy et al., 2010; Mellon et al., 2008).

All sites exhibiting probable fracture control on the clastic patterns are located on the plains beyond the ejecta of Lomonosov crater. This region has more fracture patterns than the crater interior, so more environments where fracture control can occur. There are only three images where all of the boulder halos appear to exhibit fracture control: all of the sites within ESP_026850_2475 appear to be fracture controlled. These features consist of clastic networks ranging from grade 1 to grade 3. Some of these features include coherent lines of clasts following the underlying fractures. The same is found in PSP_001520_2470, where both boulder clusters (grade 2 and 3 respectively) exhibit a degree of fracture control. However, in this instance the fractures are much fainter. TRA_000846_2475 is the only other image where all of the sites appear fracture controlled, but here all of the sites within the image are grade 2 and so do not suggest a very strong likelihood that sorting is present in the first place.

Several other images have a few boulder patches which appear to exhibit fracture control, usually corresponding to patches with low sorting grades. The only grade four site to exhibit fracture control is in ESP_025294_2415, to the south of Lomonosov crater. This site overlays faint fractures, which are more pronounced elsewhere in the image. Here the discontinuous net definitely reflects the underlying fracture pattern. One other site in this image contains a grade four net with underlying fractures, but here there is less well-expressed fracture control. PSP_010051_2435 contains a grade four discontinuous clastic net with possible fracture control from the faint underlying polygons, but here it is impossible to be certain that the fractures and the clastic net are consistent in orientation and location.

4.2. Boulder ratcheting or gravitational sorting?

The two fracture control mechanisms would produce a different arrangement of clasts. If gravitational sorting predominates then clasts would be expected to be found inside troughs or overlying fractures. If boulder ratcheting produces the arrangements then

Table 6
Summary of results of the analysis to determine how many sites exhibited fracture control.

Presence of fractures	Number of sites	Percentage of total
No fractures	55	37.42
Fractures uncertain	7	4.76
Fractures present	85	57.82
Total	147	
Relationship between clast and fracture patterns	**Number of sites**	**Percentage of sites with fractures**
No relationship	36	39.13
Uncertain relationship	35	38.04
clear relationship	21	22.83
Total	92	
Total sites without fracture control	**Number of sites**	**Percentage of total**
	91	61.90

Table 7
Summary of results.

HiRISE image	Boulder clusters	Showing organisation	Max sorting grade	Fractures present	Fracture control evident	Description
ESP_017580_2460	21	21	3	2	2 possible	Clasts by fractures
ESP_027918_2455	1	1	3	0	0	Lines of clasts
PSP_007440_2455	3	3	4	3	1 possible	Discontinuous net
PSP_010644_2455	14	14	4	0	0	Discontinuous net
ESP_026441_2460	9	8	2	1	0	Discontinuous net
TRA_000846_2475	3	3	3	3	3 certain	Lines of clasts
ESP_017131_2485	27	14	2	26	9 possible, 1 certain	Possible clustering
ESP_017632_2475	28	20	4	23	15 possible, 1 certain	Discontinuous net
ESP_019900_2470	1	1	3	1	1 certain	Lines of clasts
ESP_026850_2475	5	5	5	5	5 certain	Clastic stripes
ESP_025769_2435	1	0	3	0	0	Lines of clasts
PSP_010051_2435	6	6	3	5	1 possible, 2 certain	Faint net
PSP_001520_2470	2	2	4	2	2 certain	Discontinuous net
ESP_023738_2415	6	4	0	4	3 possible	No sorting
ESP_025294_2415	10	10	4	5	3 possible, 2 certain	Possible stripes
ESP_017079_2410	8	7	3	8	1 possible, 4 certain	Clasts by fractures
ESP_026441_2460	2	2	3	0	0	No sorting

Table 8
Fracture control assessment.

Grade	Description	All sites	With fractures	Without fractures	Fracture control	No relationship	HiRISE images
0	No evidence of organisation	26	21	4	0	23	6
1	Uncertain clustering	32	27	2	6	9	7
2	Clustering of clasts	38	23	15	9	21	13
3	Clear lines and arcs	35	10	22	5	25	12
4	Discontinuous net	15	3	12	1	12	4
5	Continuous net	1	1	0	0	1	1
	Total :	147	85	55	21	91	17
	%:	100	58	37	14	62	

Table 9
Categorisation of fracture control relationships around Lomonosov crater.

Clast–fracture relationship	Number of sites
Clustering between fractures	41
Clasts in troughs	4
Uncertain	11

boulder patterns would be expected to follow the lines of fractures, but not to overlay them.

In order to evaluate whether either of these situations predominates within the fracture controlled sites the relationship between clasts and fractures was characterised. Of the sites where fracture control might have been present, the likelihood of fracture control was assessed and the type of relationship categorised (Table 9).

It can be seen that the majority of sites where fracture control is possible have a tendency for clasts to be clustered between or around the fractures, rather than overlaying or within them. Sites where clasts can be seen to be in troughs are scarce, although these are more likely to be definite fracture control sites, due to the clearer relationship making it easier to evaluate whether they are related. Many of the sites where boulders are clustered between fractures are categorised as possibly exhibiting fracture control, but this is often uncertain.

This would seem to suggest that a boulder ratcheting hypothesis is more likely to explain sites where fracture control is evident. However, the generally low proportion of sites where fracture control is likely means that these features may simply occur through chance. Many sites have uncertain fracture control; relatively few have a definite relationship between the positions of the clasts and the underlying fracture pattern. Table 10 lists all instances of possible fracture control and describes the type of relationship observed.

5. Conclusions

Examples of putative clastic patterned ground were observed across the study area. Low graded patterned ground was ubiqui-

Table 10
List of sites with possible fracture control

Id	Sorting grade	Fracture control	Description	HiRISE image
18	1	Possible	Uncertain	ESP_017580_2460
19	2	Possible	Clustering between fractures	ESP_017580_2460
23	3	Possible	Uncertain	PSP_007440_2455
49	2	Yes	Clustering between fractures	TRA_000846_2475
50	2	Yes	Clustering between fractures	TRA_000846_2475
51	2	Yes	Clustering between fractures	TRA_000846_2475
55	2	Possible	Clustering between fractures	ESP_017131_2485
56	2	Possible	Clustering between fractures	ESP_017131_2485
66	1	Possible	Uncertain	ESP_017131_2485
70	2	Possible	Clustering between fractures	ESP_017131_2485
71	2	Possible	Uncertain	ESP_017131_2485
72	2	Possible	Clustering between fractures	ESP_017131_2485
73	2	Possible	Uncertain	ESP_017131_2485
75	0	Possible	Clustering between fractures	ESP_017131_2485
77	1	Yes	Clustering between fractures	ESP_017131_2485
78	1	Possible	Uncertain	ESP_017131_2485
79	1	Possible	Uncertain	ESP_017632_2475
80	2	Possible	Clustering between fractures	ESP_017632_2475
88	1	Possible	Uncertain	ESP_017632_2475
89	1	Possible	Clustering between fractures	ESP_017632_2475
90	1	Possible	Uncertain	ESP_017632_2475
91	1	Possible	Clustering between fractures	ESP_017632_2475
92	1	Possible	Clustering between fractures	ESP_017632_2475
94	1	Possible	Clustering between fractures	ESP_017632_2475
95	1	Possible	Clustering between fractures	ESP_017632_2475
96	1	Possible	Clustering between fractures	ESP_017632_2475
99	1	Possible	Clustering between fractures	ESP_017632_2475
102	1	Possible	Clustering between fractures	ESP_017632_2475
103	0	Possible	Clustering between fractures	ESP_017632_2475
104	1	Possible	Clustering between fractures	ESP_017632_2475
105	1	Possible	Clustering between fractures	ESP_017632_2475
106	1	Yes	Clustering between fractures	ESP_017632_2475
107	3	Yes	Clustering between fractures	ESP_019900_2470
108	1	Yes	Clustering between fractures	ESP_02850_2475
109	3	Yes	Clustering between fractures	ESP_02850_2475
110	1	Yes	Clustering between fractures	ESP_02850_2475
111	1	Yes	Clustering between fractures	ESP_02850_2475
112	2	Yes	Clustering between fractures	ESP_02850_2475
114	2	Yes	Clustering between fractures	PSP_010051_2435
117	2	Yes	Clustering between fractures	PSP_010051_2435
118	4	Possible	Clustering between fractures	PSP_010051_2435
120	3	Yes	Boulders follow fractures	PSP_001520_2470
121	2	Yes	Clustering between fractures	PSP_001520_2470
122	3	Possible	Uncertain	ESP_023738_2415
126	0	Possible	Possibly clasts in troughs	ESP_023738_2415
127	3	Possible	Clustering between fractures	ESP_023738_2415
128	4	Possible	Clustering between fractures	ESP_025294_2415
129	4	Yes	Clustering between fractures	ESP_025294_2415
134	3	Possible	Clustering between fractures	ESP_025294_2415
135	2	Yes	Clustering between fractures	ESP_025294_2415
136	3	Possible	Uncertain	ESP_025294_2415
140	3	Yes	Clasts in troughs	ESP_017079_2410
141	3	Yes	Clasts in troughs	ESP_017079_2410
143	2	Yes	Clasts in troughs	ESP_017079_2410
144	1	Possible	Clustering between fractures	ESP_017079_2410
145	1	Yes	Clustering between fractures	ESP_017079_2410

tous in the HiRISE images examined, while more strongly organised sites were less common. It is interesting that the locations with highly graded patterns are not restricted to the crater interior, and are in fact scattered quite widely across the study area. They occur within a variety of different terrains ranging from the flat ground of the Northern Plains to the steeper slopes of crater walls. The presence of the same landforms in widely spaced images would seem to suggest that whatever process is responsible for their formation is occurring across the area, rather than being limited to one or more unusual micro-environments.

It was found that the majority of sites examined in the Lomonosov area did not exhibit a relationship between apparently organized clastic patterns and thermal contraction fracture networks. Fractures were present at a large number of sites, but did not appear to be substantially influencing the arrangement of clasts. Furthermore, a larger number of boulder patches exhibiting higher grade sorting were found at sites with no evidence of fracture control. Thus, although these fracture-control hypotheses cannot be completely ruled out, it seems unlikely that they account for the observed organisation of clasts into network-like patterns.

There is a substantial amount of uncertainty involved in any remote sensing study, and this must be acknowledged when considering the results of this investigation. Although fracture control does not appear to be prevalent at this site it is impossible to be certain how these features formed from the currently available data. Higher resolution images, or ideally in-situ observations would be required to definitively rule out a fracture controlled scenario.

That said, the absence of a clear fracture controlled arrangement suggests that a different mechanism would most likely be required to shape the development of these patterns. One theory is that these features might result from periglacial freeze-thaw sorting, possibly augmented by the presence of cryobrines. The lack of fracture controlled arrangements at this site leaves open the possibility of a periglacial formation mechanism, however the rejection of these alternate hypotheses is not intended to address competing models. Further investigations are required to evaluate the remaining model, and it is always possible that an as yet unknown mechanism could be responsible for the development of these features.

In conclusion, while fracture control may be responsible for some of the lower grade features within the study area, it is clear that the majority of the discontinuous nets across the area are not fracture controlled. In particular while the sorted stripes in ESP_017131_2485, the only large area to score a grade five on the classification scheme within this study area, do overlay a fracture net; they do not exhibit any evidence of fracture control. This is the same relationship observed by Gallagher et al., (2011) in Heimdal crater, and shows that the sorting process and the fracturing process are probably not related at these locations. Neither the frost locking nor the gravitational sorting hypotheses therefore seem likely to account for the organisation of clasts apparent in the Lomonosov crater region.

Acknowledgements

This research was funded by the UK Space Agency Aurora program, The Open University's Centre for Earth, Planetary, Space and Astronomical Research (CEPSAR) and the Science and Technology Facilities Council (STFC) (Grant number ST/L000776/1). Additionally MRP acknowledges support from the UK Space Agency (grant number ST/P001262/1) and the EU Horizon 2020 Program (UPWARDS-633127).

References

Aharonson, O., Schorghofer, N., Gerstell, M.F., 2003. Slope streak formation and dust deposition rates on Mars. J. Geophys. Res. 108, 5138. doi:10.1029/2003JE002123.

Balme, M.R., Gallagher, C., 2009. An equatorial periglacial landscape on Mars. Earth Planet. Sci. Lett. 285, 1–15. doi:10.1016/j.epsl.2009.05.031.

Balme, M.R., Gallagher, C.J., Hauber, E., 2013. Morphological evidence for geologically young thaw of ice on Mars: a review of recent studies using high-resolution imaging data. Prog. Phys. Geogr. 37, 289–324. doi:10.1177/0309133313477123.

Balme, M.R., Gallagher, C.J., Page, D.P., Murray, J.B., Muller, J.-P., 2009. Sorted stone circles in Elysium Planitia, Mars: Implications for recent Martian climate. Icarus 200, 30–38. doi:10.1016/j.icarus.2008.11.010.

Banks, M.E., McEwen, A.S., Kargel, J.S., Baker, V.R., Strom, R.G., Mellon, M.T., Gulick, V.C., Keszthelyi, L., Herkenhoff, K.E., Pelletier, J.D., Jaeger, W.L., 2008. High resolution imaging science experiment (HiRISE) observations of glacial and periglacial morphologies in the circum-Argyre Planitia highlands. Mars J. Geophys. Res. 113, E12015. doi:10.1029/2007JE002994.

Barrett, A., 2014. An Investigation of Potential Periglacial Landforms on the Northern Plains of Mars: An Integrated Field, Laboratory and Remote Sensing Study. Open University.

Christensen, P., Gorelick, N.S., Mehall, G.L., Murray, K.C., 2010. THEMIS Public Data Releases.

Clark, P.J., Evans, F.C., 1954. Distance to nearest neighbor as a measure of spatial relationships in populations. Ecology 35, 445–453.

Corte, A.E., 1963. Particle sorting by repeated freezing and thawing. Science 142, 499–501. doi:10.1126/science.142.3591.499.

Delamere, A., Becker, I., Bergstrom, J., Burkepile, J., Day, J., Dorn, D., Gallagher, D., Hamp, C., Lasco, J., Meiers, B., Sievers, A., Streetman, S., Tarr, S., Tommeraasen, M., Volmer, P., 2003. MRO high resolution imaging science experiment (HIRISE): instrument development. In: Sixth International Conference on Mars, pp. 1–4.

Delamere, W.A., Tornabene, L.L., McEwen, A.S., Becker, K., Bergstrom, J.W., Bridges, N.T., Eliason, E.M., Gallagher, D., Herkenhoff, K.E., Keszthelyi, L., Mattson, S., McArthur, G.K., Mellon, M.T., Milazzo, M., Russell, P.S., Thomas, N., 2010. Color imaging of Mars by the high resolution imaging science experiment (HiRISE). Icarus 205, 38–52. doi:10.1016/j.icarus.2009.03.012.

Dundas, C.M., McEwen, A.S., 2010. An assessment of evidence for pingos on Mars using HiRISE. Icarus 205, 244–258. doi:10.1016/j.icarus.2009.02.020.

Dutilleul, P., Haltigin, T.W., Pollard, W.H., 2009. Analysis of polygonal terrain landforms on Earth and Mars through spatial point patterns. Environmetrics 20, 206–220. doi:10.1002/env.

Feuillet, T., Mercier, D., Decaulne, A., Cossart, E., 2012. Classification of sorted patterned ground areas based on their environmental characteristics (Skagafjörður, Northern Iceland). Geomorphology 139–140, 577–587. doi:10.1016/j.geomorph.2011.12.022.

French, H., 2007. The Periglacial Environment, third ed Wiley, Chichester.

Gallagher, C., Balme, M., 2015. Eskers in a complete, wet-based glacial system in the Phlegra Montes region, Mars. Earth Planet. Sci. Lett. 431, 96–109. doi:10.1016/j.epsl.2015.09.023.

Gallagher, C., Balme, M.R., 2011. Landforms indicative of ground-ice thaw in the northern high latitudes of Mars. Geol. Soc. London, Spec. Publ. 356, 87–110. doi:10.1144/SP356.6.

Gallagher, C., Balme, M.R., Conway, S.J., Grindrod, P.M., 2011. Sorted clastic stripes, lobes and associated gullies in high-latitude craters on Mars: landforms indicative of very recent, polycyclic ground-ice thaw and liquid flows. Icarus 211, 458–471. doi:10.1016/j.icarus.2010.09.010.

Haltigin, T.W., Pollard, W.H., Dutilleul, P., Osinski, G.R., 2012. Geometric evolution of polygonal terrain networks in the Canadian High Arctic: evidence of increasing regularity over time. Permafrost Periglacial Process. 23, 178–186. doi:10.1002/ppp.1741.

Haltigin, T.W., Pollard, W.H., Dutilleul, P., Osinski, G.R., Koponen, L., 2014. Co-evolution of polygonal and scalloped terrains, southwestern Utopia Planitia, Mars. Earth Planet. Sci. Lett. 387, 44–54. doi:10.1016/j.epsl.2013.11.005.

Hauber, E., Reiss, D., Ulrich, M., Preusker, F., Trauthan, F., Zanetti, M., Hiesinger, H., Jaumann, R., Johansson, L., Johnsson, A., Van Gasselt, S., Olvmo, M., 2011a. Landscape evolution in Martian mid-latitude regions: insights from analogous periglacial landforms in Svalbard. Geol. Soc. London, Spec. Publ. 356, 111–131. doi:10.1144/SP356.7.

Hauber, E., Reiss, D., Ulrich, M., Preusker, F., Trauthan, F., Zanetti, M., Hiesinger, H., Jaumann, R., Johansson, L., Johnsson, A., Van Gasselt, S., Olvmo, M., 2011b. Landscape evolution in Martian mid-latitude regions: insights from analogous periglacial landforms in Svalbard. Geol. Soc. London, Spec. Publ. 356, 111–131. doi:10.1144/SP356.7.

Hecht, M., 2002. Metastability of liquid water on Mars. Icarus 156, 373–386. doi:10.1006/icar.2001.6794.

Johnsson, A., Reiss, D., Hauber, E., Zanetti, M., Hiesinger, H., Johansson, L., Olvmo, M., 2012. Periglacial mass-wasting landforms on Mars suggestive of transient liquid water in the recent past: insights from solifluction lobes on Svalbard. Icarus 218, 489–505. doi:10.1016/j.icarus.2011.12.021.

Kessler, M.A., Murray, A.B., Werner, B.T., Hallet, B., 2001. A model for sorted circles as self-organized patterns. J. Geophys. Res. 106, 13287. doi:10.1029/2001JB000279.

Kessler, M.A., Werner, B.T., 2003. Self-organization of sorted patterned ground. Science 299, 380–383. doi:10.1126/science.1077309.

Kieffer, H.H., Jakosky, B.M., Snyder, C.W., Matthews, M.S., 1992. Mars. University of Arizona Press, Tucson.

Krantz, W.B., 1990. Self-organization manifest as patterned ground in recurrently frozen soils. Earth-Sci. Rev 29, 117–130. doi:10.1016/0012-8252(90)90031-P.

Lachenbruch, A.H., 1962. Mechanics of thermal contraction cracks and ice-wedge polygons in permafrost. Geol. Soc. Am. Spec. Pap. 70, 69.

Landis, G.A., Jenkins, P.P., 2000. Measurement of the settling rate of atmospheric dust on Mars by the MAE instrument on Mars Pathfinder. J. Geophys. Res. 105, 1855–1858.

Levy, J.S., Head, J., Marchant, D., 2009a. Thermal contraction crack polygons on Mars: classification, distribution, and climate implications from HiRISE observations. J. Geophys. Res. 114, 1–19. doi:10.1029/2008JE003273.

Levy, J.S., Head, J.W., Marchant, D.R., 2008a. Origin and arrangement of boulders on the Martian Northern Plains: assessment of emplacement and modification environments. In: Lunar and Planetary Science XXXIX (2008), pp. 1–2. doi:10.1029/2005GL024360.

Levy, J.S., Head, J.W., Marchant, D.R., Dickson, J.L., Morgan, G.A., 2009b. Geologically recent gully–polygon relationships on Mars: insights from the Antarctic Dry Valleys on the roles of permafrost, microclimates, and water sources for surface flow. Icarus 201, 113–126. doi:10.1016/j.icarus.2008.12.043.

Levy, J.S., Head, J.W., Marchant, D.R., Kowalewski, D.E., 2008b. Identification of sublimation-type thermal contraction crack polygons at the proposed NASA Phoenix landing site: implications for substrate properties and climate-driven morphological evolution. Geophys. Res. Lett 35, L04202. doi:10.1029/2007GL032813.

Levy, J.S., Marchant, D.R., Head, J.W., 2010. Thermal contraction crack polygons on Mars: a synthesis from HiRISE, Phoenix, and terrestrial analog studies. Icarus 206, 229–252. doi:10.1016/j.icarus.2009.09.005.

Malin, M.C., Edgett, K.S., 2001. Mars global surveyor Mars orbiter camera: interplanetary cruise through primary mission. J. Geophys. Res. 106, 23429. doi:10.1029/2000JE001455.

Mangold, N., 2005. High latitude patterned grounds on Mars: classification, distribution and climatic control. Icarus 174, 336–359. doi:10.1016/j.icarus.2004.07.030.

Marion, G.M., Catling, D.C., Zahnle, K.J., Claire, M.W., 2010. Modeling aqueous perchlorate chemistries with applications to Mars. Icarus 207, 675–685. doi:10.1016/j.icarus.2009.12.003.

Matsuoka, N., Abe, M., Ijiri, M., 2003. Differential frost heave and sorted patterned ground: field measurements and a laboratory experiment. Geomorphology 52, 73–85. doi:10.1016/S0169-555X(02)00249-0.

McEwen, A.S., Banks, M.E., Baugh, N., Becker, K., Boyd, A., Bergstrom, J.W., Beyer, R.a., Bortolini, E., Bridges, N.T., Byrne, S., Castalia, B., Chuang, F.C., Crumpler, L.S., Daubar, I., Davatzes, A.K., Deardorff, D.G., DeJong, A., Alan Delamere, W., Dobrea, E.N., Dundas, C.M., Eliason, E.M., Espinoza, Y., Fennema, A., Fish-

baugh, K.E., Forrester, T., Geissler, P.E., Grant, J.a., Griffes, J.L., Grotzinger, J.P., Gulick, V.C., Hansen, C.J., Herkenhoff, K.E., Heyd, R., Jaeger, W.L., Jones, D., Kanefsky, B., Keszthelyi, L., King, R., Kirk, R.L., Kolb, K.J., Lasco, J., Lefort, A., Leis, R., Lewis, K.W., Martinez-Alonso, S., Mattson, S., McArthur, G., Mellon, M.T., Metz, J.M., Milazzo, M.P., Milliken, R.E., Motazedian, T., Okubo, C.H., Ortiz, A., Philippoff, A.J., Plassmann, J., Polit, A., Russell, P.S., Schaller, C., Searls, M.L., Spriggs, T., Squyres, S.W., Tarr, S., Thomas, N., Thomson, B.J., Tornabene, L.L., Van Houten, C., Verba, C., Weitz, C.M., Wray, J.J., 2010. The high resolution imaging science experiment (HiRISE) during MRO's primary science phase (PSP). Icarus 205, 2–37. doi:10.1016/j.icarus.2009.04.023.

Mellon, M.T., 1997. Small-scale polygonal features on Mars: seasonal thermal contraction cracks in permafrost. J. Geophys. Res. 102, 25617. doi:10.1029/97JE02582.

Mellon, M.T., Arvidson, R.E., Marlow, J.J., Phillips, R.J., Asphaug, E., 2008. Periglacial landforms at the Phoenix landing site and the Northern Plains of Mars. J. Geophys. Res. 113, 1–15. doi:10.1029/2007JE003039.

Nicholson, F.H., 1976. Patterned ground formation and description as suggested by low Arctic and subarctic examples. Arct. Alp. Res. 8, 329–342.

Ojha, L., Wilhelm, M.B., Murchie, S.L., McEwen, A.S., Wray, J.J., Hanley, J., Massé, M., Chojnacki, M., 2015. Spectral evidence for hydrated salts in recurring slope lineae on Mars. Nat. Geosci. doi:10.1038/ngeo2546.

Orloff, T., Kreslavsky, M., Asphaug, E., Korteniemi, J., 2011. Boulder movement at high northern latitudes of Mars. J. Geophys. Res. 116, 1–12. doi:10.1029/2011JE003811.

Orloff, T.C., 2012. Geomorphological Analysis of Boulders and Polygons on Martian Periglacial Patterned Ground Terrains. University of California, Santa Cruz.

Orloff, T.C., Kreslavsky, M.A., Asphaug, E.I., 2013. Possible mechanism of boulder clustering on Mars. Icarus 225, 992–999. doi:10.1016/j.icarus.2013.01.002.

Rossi, A.P., Van Gasselt, S., Pondrelli, M., Dohm, J., Hauber, E., Dumke, A., Zegers, T., Neukum, G., 2011. Evolution of periglacial landforms in the ancient mountain range of the Thaumasia Highlands, Mars. Geol. Soc. London, Spec. Publ. 356, 69–85. doi:10.1144/SP356.5.

Ruff, S.W., 2002. Bright and dark regions on Mars: particle size and mineralogical characteristics based on Thermal Emission Spectrometer data. J. Geophys. Res. 107, 5127. doi:10.1029/2001JE001580.

Séjourné, A., Costard, F., Gargani, J., Soare, R.J., Fedorov, A., Marmo, C., 2011. Scalloped depressions and small-sized polygons in western Utopia Planitia, Mars: a new formation hypothesis. Planet. Space Sci. 59, 412–422. doi:10.1016/j.pss.2011.01.007.

Smith, E., Zuber, M.T., Frey, V., Garvin, B., Muhleman, O., Pettengill, H., Phillips, J., Solomon., S.C., Zwally, H.J., Banerdt, W.B., Duxbury, C., Golombek, M.P., Lemoine, G., Neumann, G.A., Rowlands, D.D., Aharonson, O., Ford, P.G., Ivanov, A.B., Johnson, C.L., McGovern, J., Abshire, B., Afzal, R.S., Sun, X., 2001. Mars orbiter laser altimeter : experiment summary after the first year of global mapping of Mars. J. Geophys. Res. 106, 689–722.

Soare, R., Conway, S.J., Gallagher, C., Dohm, J.M., 2016. Sorted (clastic) polygons in the Argyre region, Mars, and possible evidence of pre-and post- glacial periglaciation in the Late Amazonian Epoch. Icarus 264, 184–197.

Soare, R.J., Burr, D.M., Wan Bun Tseung, J.M., 2005. Possible pingos and a periglacial landscape in northwest Utopia Planitia. Icarus 174, 373–382. doi:10.1016/j.icarus.2004.11.013.

Soare, R.J., Conway, S.J., Dohm, J.M., 2014. Possible ice-wedge polygons and recent landscape modification by "wet" periglacial processes in and around the Argyre impact basin. Mars Icarus 233, 214–228. doi:10.1016/j.icarus.2014.01.034.

Soare, R.J., Conway, S.J., Gallagher, C., Dohm, J.M., 2016. Sorted (clastic) polygons in the Argyre region, Mars, and possible evidence of pre- and post-glacial periglaciation in the Late Amazonian Epoch. Icarus 264, 184–197. doi:10.1016/j.icarus.2015.09.019.

Soare, R.J., Sejourne, A., Pearce, G., Costard, F., Osinski, G.R., 2011. The Tuktoyaktuk coastlands of northern Canada: a possible "wet" periglacial analog of Utopia Planitia. Mars Analog. Planet. Explor. 203–218. doi:10.1130/2011.2483(13).

Tanaka, K.L., Skinner, J.A., Hare, T.M., 2005. Geologic Map of the Northern Plains of Mars. 1:15, 000, 000, US Geological Survey Scientific Investigations Map 2888.

Ulrich, M., Hauber, E., Herzschuh, U., Härtel, S., Schirrmeister, L., 2011. Polygon pattern geomorphometry on Svalbard (Norway) and Western Utopia Planitia (Mars) using high-resolution stereo remote-sensing data. Geomorphology 134, 197–216. doi:10.1016/j.geomorph.2011.07.002.

Ulrich, M., Wagner, D., Hauber, E., de Vera, J.-P., Schirrmeister, L., 2012. Habitable periglacial landscapes in Martian mid-latitudes. Icarus 219, 345–357. doi:10.1016/j.icarus.2012.03.019.

Washburn, A.L., 1956. Classification of patterned ground and review of suggested origins. Geol. Soc. Am. Bull. 67, 823–866. doi:10.1130/0016-7606(1956)67.

Washburn, A.L., 1973. Periglacial Processes and Environments. Edward Arnold.